frontiers | Frontiers in Neurology

TYPE Original Research
PUBLISHED 23 December 2024
DOI 10.3389/fneur.2024.1482892

OPEN ACCESS

EDITED BY
Walter Marcotti,
The University of Sheffield, United Kingdom

REVIEWED BY
Corné Kros,
University of Sussex, United Kingdom
Philippe Vincent,
Johns Hopkins Medicine, United States

*CORRESPONDENCE
A. Catalina Vélez-Ortega
✉ catavelezo@uky.edu

RECEIVED 19 August 2024
ACCEPTED 03 December 2024
PUBLISHED 23 December 2024

CITATION
López-Porras AI, Kruse AM, McClendon MT and Vélez-Ortega AC (2024) Myosin XVA isoforms participate in the mechanotransduction-dependent remodeling of the actin cytoskeleton in auditory stereocilia.
Front. Neurol. 15:1482892.
doi: 10.3389/fneur.2024.1482892

Myosin XVA isoforms participate in the mechanotransduction-dependent remodeling of the actin cytoskeleton in auditory stereocilia

Ana I. López-Porras, Ava M. Kruse, Mark T. McClendon and A. Catalina Vélez-Ortega*

Department of Physiology, University of Kentucky, Lexington, KY, United States

Auditory hair cells form precise and sensitive staircase-like actin protrusions known as stereocilia. These specialized microvilli detect deflections induced by sound through the activation of mechano-electrical transduction (MET) channels located at their tips. At rest, a small MET channel current results in a constant calcium influx which regulates the morphology of the actin cytoskeleton in the shorter 'transducing' stereocilia. However, the molecular mechanisms involved in this novel type of activity-driven plasticity in the stereocilium cytoskeleton are currently unknown. Here, we tested the contribution of myosin XVA (MYO15A) isoforms, given their known roles in the regulation of stereocilia dimensions during hair bundle development and the maintenance of transducing stereocilia in mature hair cells. We used electron microscopy to evaluate morphological changes in the cytoskeleton of auditory hair cell stereocilia after the pharmacological blockage of resting MET currents in cochlear explants from mice that lacked one or all isoforms of MYO15A. Hair cells lacking functional MYO15A isoforms did not exhibit MET-dependent remodeling in their stereocilia cytoskeleton. In contrast, hair cells lacking only the long isoform of MYO15A exhibited increased MET-dependent stereocilia remodeling, including remodeling in stereocilia from the tallest 'non-transducing' row of the bundle. We conclude that MYO15A isoforms both enable and fine-tune the MET-dependent remodeling of the actin cytoskeleton in transducing stereocilia, while also contributing to the stability of the tallest row.

KEYWORDS

myosin XVA, hair cells, stereocilia, actin cytoskeleton, remodeling, mechanotransduction

1 Introduction

Inner ear hair cells have modified microvilli, known as stereocilia, on their apical surfaces. Stereocilia are arranged into highly organized bundles with rows of increasing height in a staircase manner. The cytoskeleton within each stereocilium contains hundreds of parallel and polarized actin filaments that are highly crosslinked, resulting in a rather rigid, paracrystalline arrangement (1–4). The tips of shorter stereocilia are connected to the shafts of their taller neighbors via extracellular tip links, thus stereocilia bundle deflections in the direction of the tallest row increase the tension at the tips of shorter stereocilia (5, 6) where mechano-electrical transduction (MET) channels are located (7). MET channels are non-selective cation channels

(8, 9). To maintain the sensitivity of the hair bundle, tip links are kept under tension even at rest, which results in the constant entry of calcium into stereocilia (9, 10). We and others previously showed that this resting calcium entry impacts the morphology of the stereocilia cytoskeleton. In our previous study, we used (*i*) MET channel blockers, (*ii*) disruption of tips links, and (*iii*) manipulations of intracellular and extracellular calcium to show that a decrease in the resting calcium entry leads to the thinning of stereocilia tips and their eventual shortening (11). Conversely, an increase in resting calcium entry leads to thickening of the stereocilia tips while removal of MET channel blockers or tip link regeneration induces stereocilia regrowth (11). During the postnatal development of the hair bundle in the mouse, MET currents (and/or components of the MET machinery) are essential to establish correct stereocilia dimensions (height and thickness) in all rows of the bundle (12, 13). Mechanotransduction is also required for the proper trafficking of certain stereocilia tip proteins that are differentially expressed between the tallest and the shorter stereocilia, collectively known as 'row-identity' proteins (12–14). Altogether, these findings highlight a clear interplay between MET activity and stereocilia cytoskeleton remodeling. However, the exact molecular machinery involved in this process is still unknown. This study explores whether MYO15A—the master protein regulating stereocilia elongation during hair cell bundle development—is involved in the MET-dependent remodeling of the actin cytoskeleton within mammalian auditory stereocilia.

MYO15A is a non-conventional myosin that localizes to the tips of stereocilia (15). It delivers proteins required for the proper elongation of the stereocilium actin core, such as: the scaffolding protein WHRN (16), the actin capping/bundling protein EPS8 (17), and the GPSM2-GNAI3 signaling complex (18). Functional defects in MYO15A, WHRN, EPS8, GPSM2 or GNAI3 all lead to profound hearing loss and abnormally short stereocilia in auditory hair cells (17–20). Three isoforms of MYO15A have been identified in the auditory hair cells (15, 21–23), but only two of them have been characterized in detail in the mouse. The shortest isoform, MYO15A-2, exhibits elevated mRNA levels at birth that quickly decline. As a protein, MYO15A-2 is preferentially trafficked to the tips of stereocilia from the tallest row of the bundle. MYO15A-1 is the longest isoform due to the addition of a large (~130 kDa) N-terminal domain. MYO15A-1 mRNA levels continually increase during the first postnatal weeks and, as a protein, this isoform is preferentially trafficked to the tips of stereocilia from the shorter rows of the bundle. The third isoform, MYO15A-3, has a unique small N-terminal domain making it intermediate in size. However, its localization within the hair cell bundle remains to be characterized.

In *shaker-2* mice ($Myo15a^{sh2/sh2}$), a point mutation in the motor domain of MYO15A renders all isoforms non-functional (i.e., unable to reach the stereocilia tips) (15) and while stereocilia are abnormally short (20) they still exhibit MET currents (24, 25). In mice lacking the long isoform of MYO15A only ($Myo15a^{\Delta N/\Delta N}$), auditory hair cells develop normally, exhibit nearly normal MET currents, but their shorter ('transducing') stereocilia degenerate prematurely (26). Here, we evaluated the MET-dependent remodeling of the stereocilia cytoskeleton in auditory hair cells from $Myo15a^{sh2/sh2}$ and $Myo15a^{\Delta N/\Delta N}$ mice. Our results indicate that MYO15A is essential to deliver the machinery involved in MET-dependent stereocilia remodeling. In addition, the long isoform of MYO15A also delivers machinery that provides cytoskeleton stability.

2 Results

2.1 MYO15A is required for the MET-dependent remodeling of the stereocilia cytoskeleton

We previously showed that blockage of the resting MET current with pharmacological MET channel blockers like tubocurarine (27) or benzamil (28) induces the remodeling of the stereocilium cytoskeleton in auditory hair cells (11). To test the role of MYO15A in this MET-dependent remodeling of stereocilia, we used *shaker-2* mice which have a recessive point mutation in the motor domain of MYO15A that renders all known isoforms unable to climb the stereocilia tips. While the *shaker-2* hair cell bundles are abnormally short, *shaker-2* auditory hair cells still exhibit MET currents, including currents at resting bundle positions (24, 25). Therefore, we used MET channel blockage to evaluate the remodeling of neonate auditory stereocilia from heterozygous ($Myo15a^{+/sh2}$) and homozygous ($Myo15a^{sh2/sh2}$) *shaker-2* littermates.

As expected, 300 μM of tubocurarine significantly reduced the uptake of the FM1-43 dye through MET channels open at rest in inner and outer hair cells (IHC and OHC, respectively) from heterozygous and homozygous *shaker-2* mice at postnatal day 5 (P5) (Figure 1A). After 4 h of MET channel blockage with 300 μM of tubocurarine, scanning electron microscopy (SEM) images showed significant thinning of second row stereocilia tips in postnatal day 5 (P5) heterozygous but not homozygous OHC (Figures 1B,C). In addition to the stereocilia thinning, significant stereocilia shortening was observed in second and third row stereocilia from heterozygous but not homozygous mice (Figure 1D). In our previous study (11), we found that MET channel blockage does not affect the morphology of stereocilia from the tallest row in wild-type bundles, which do not express MET channels (7). Similarly, here we found no signs of shortening in stereocilia from the tallest row in OHC from either heterozygous or homozygous *shaker-2* mice (Figure 1D).

As previously reported, MET channel blockage also leads to the remodeling of the actin cytoskeleton in transducing stereocilia of IHC (11). In heterozygous *shaker-2* IHC, SEM images showed thinning of stereocilia from the second row of the bundle (Figures 2A,B). Stereocilia shortening was also observed in the third row of the bundle (Figure 2C), but no morphological changes were observed in stereocilia from the tallest row (Figures 2A,C). In contrast, homozygous *shaker-2* IHC showed no evidence of cytoskeleton remodeling in stereocilia from the first, second, or third rows of the bundle (Figures 2A–C). Homozygous *shaker-2* IHC stereocilia are not only abnormally short but they also lack a staircase arrangement (25, 29) thus obtaining stereocilia height measurements from SEM images is rather challenging. Therefore, we also performed focused ion beam SEM (FIB-SEM) to obtain cross-sections of IHC stereocilia bundles and more accurate measurements of stereocilia heights from homozygous *shaker-2* IHC cells cultured in control conditions or with 60 or 300 μM of tubocurarine for 4–5.5 h (Figure 2D). Once again, MET channel blockage did not lead to shortening of stereocilia from the first or second rows of the bundle in homozygous *shaker-2* IHC cells (Figure 2E).

Our previous study (11) showed quantitatively larger stereocilia remodeling in OHC than in IHC with concentrations of blockers

10.3389/fneur.2024.1482892

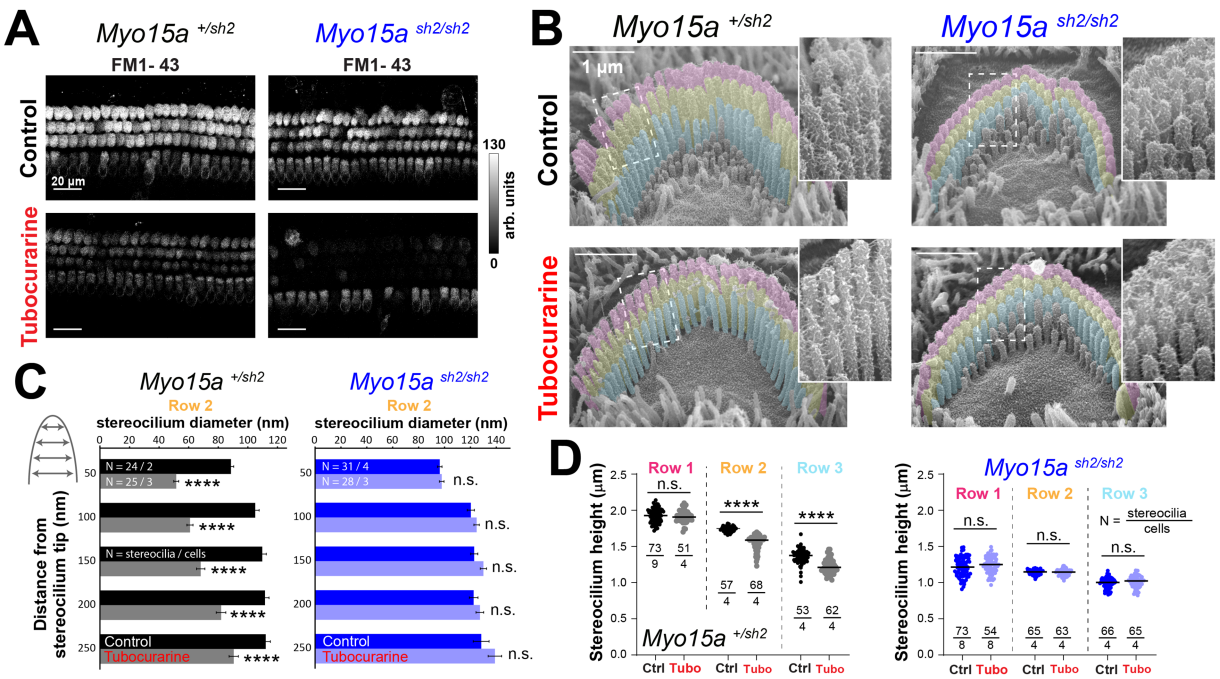

FIGURE 1
Outer hair cells lacking functional MYO15A do not exhibit mechanotransduction-dependent stereocilia remodeling. **(A)** Decreased FM1-43 dye uptake in hair cells after application of the MET channel blocker, tubocurarine (300 µM), in heterozygous (*left*) and homozygous *shaker2* (*right*) cochlear explants. **(B)** Representative false-colored scanning electron microscopy (SEM) images of outer hair cell (OHC) stereocilia bundles cultured for 4 h at 37°C in control conditions (*top*) or with 300 µM tubocurarine (*bottom*), from heterozygous control (*left*) or homozygous *shaker2* (*right*) littermates. Insets show highlighted bundle regions at higher magnification. **(C)** Diameter of stereocilia from the second row [colored in yellow in panel **(B)**] at several positions from the stereocilium tip (as indicated in cartoon), from OHC of control heterozygous (black, gray) or homozygous *shaker2* (dark and light blue) littermates cultured in control conditions (darker bars) or with tubocurarine (lighter bars). Data are shown as mean ± SE. Statistical differences were analyzed using a linear mixed model. **(D)** Heights of stereocilia from the first, second and third rows [colored in pink, yellow and cyan in panel **(B)**, respectively] of OHC from control heterozygous (black, gray) or homozygous *shaker2* (dark and light blue) littermates cultured in control conditions (darker points) or with tubocurarine (lighter points). Horizontal lines indicate the mean and statistical differences were obtained using Welch's *t* test. For all panels, the age of explants is P5, and statistical significance is shown as: **p* < 0.05, ***p* < 0.01, ****p* < 0.001, *****p* < 0.0001; n.s., not significant.

expected to reduce MET currents by ~80–90% (e.g., 30 µM of tubocurarine). Here, using a 10× higher concentration of tubocurarine (300 µM, a saturating level) we achieved somewhat larger remodeling in transducing stereocilia from IHC, which is more similar to the extent observed in OHC (compare Figure 1 to Figure 2). This larger IHC remodeling, however, did not appear to be a pharmacological side effect triggered by higher tubocurarine concentrations since no evidence of stereocilia remodeling was observed in auditory hair cells from *Cib2* mutant mice lacking normal-polarity MET currents (Supplementary Figures 1, 2) (30).

To confirm the lack of MET-dependent stereocilia remodeling in the absence of functional MYO15A, we tested the effects of MET channel blockage on IHC and OHC from heterozygous and homozygous *shaker-2* mice after (*i*) a longer incubation period (8 h, Supplementary Figures 3A,B, 4A,B), (*ii*) a younger developmental age (P4, Supplementary Figures 3C,D, 4C,D), or (*iii*) a different MET channel blocker (30 µM of benzamil for 5 h, Supplementary Figures 3E,F, 4E,F). We also tested the effect of increased intracellular calcium buffering on stereocilia actin remodeling by culturing cells with the membrane-permeable calcium chelator BAPTA-AM (20 µM for 5 h, Supplementary Figures 3E,F, 4E,F). Here and in our previous study, the effects of increased intracellular calcium buffering resembled those obtained with MET channel blockers (11). In all these conditions, MET-dependent stereocilia remodeling was evident in transducing stereocilia from heterozygous but not homozygous *shaker-2* mice.

We conclude that MYO15A is required for the delivery of the molecular machinery that enables the remodeling of the stereocilia cytoskeleton in both IHC and OHC in response to changes in the influx of calcium through MET channels that are partially open at rest.

2.2 Transducing stereocilia exhibit exaggerated MET-dependent remodeling in the absence of the long isoform of MYO15A

Next, we sought out to explore whether the long isoform of MYO15A, which is typically enriched at the tips of transducing stereocilia (26), is involved in the MET-dependent remodeling of the stereocilia cytoskeleton. We used mice lacking the long isoform of MYO15A (*Myo15a* $^{\Delta N/\Delta N}$) which develop hair cell bundles with near normal staircase arrangements and MET currents (including resting currents) (26). These mice, however, exhibit progressive hearing loss and degeneration of stereocilia in the shorter rows of the bundle.

10.3389/fneur.2024.1482892

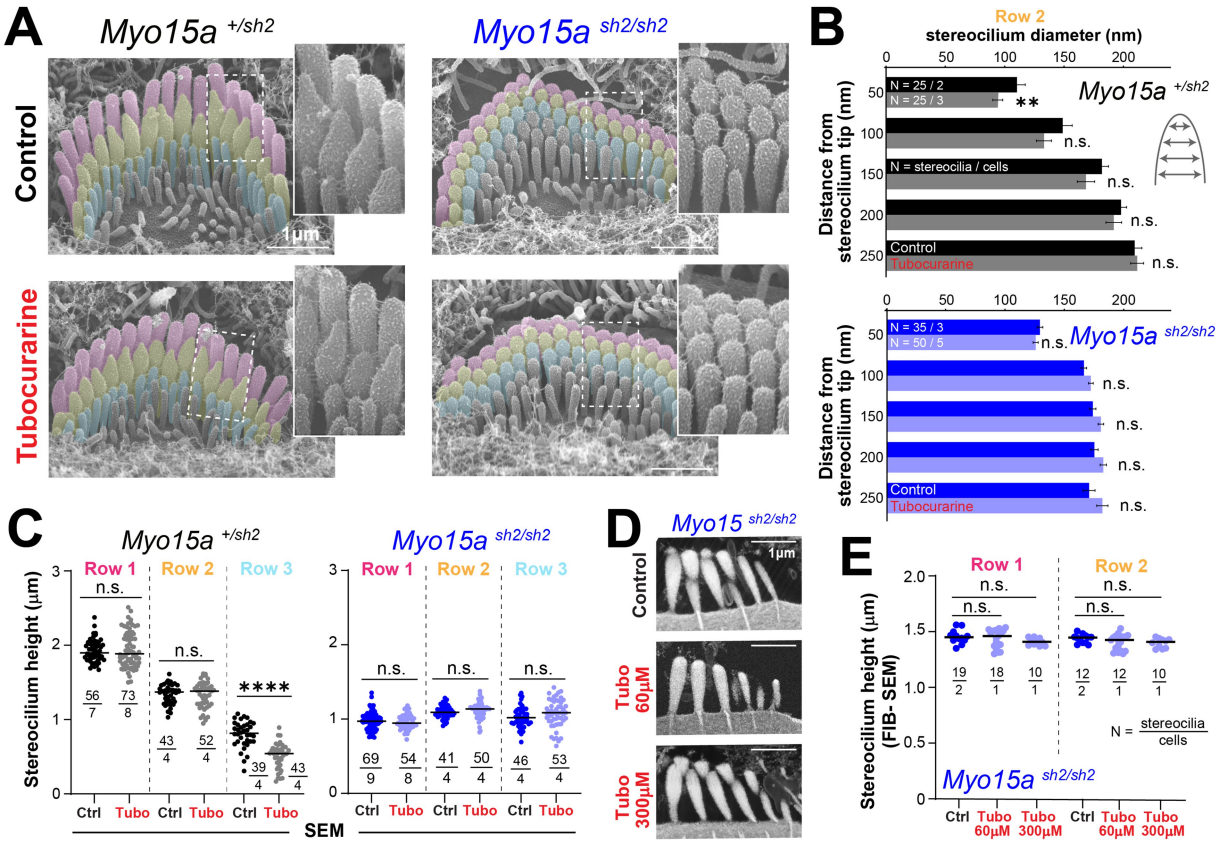

FIGURE 2
Inner hair cells lacking functional MYO15A do not exhibit mechanotransduction-dependent stereocilia remodeling. **(A)** Representative false-colored SEM images of inner hair cell (IHC) stereocilia bundles cultured for 4 h at 37°C in control conditions (*top*) or with 300 µM tubocurarine (*bottom*), from heterozygous (*left*) or homozygous *shaker2* (*right*) littermates. Insets show highlighted bundle regions at higher magnification. **(B)** Diameter of stereocilia from the second row [colored in yellow in panel **(A)**] at several positions from the stereocilium tip (as indicated in cartoon), from IHC of control heterozygous (black, gray) or homozygous *shaker2* (dark and light blue) littermates cultured in control conditions (darker bars) or with tubocurarine (lighter bars). Data are shown as mean ± SE. Statistical differences were analyzed using a linear mixed model. **(C)** Heights of stereocilia from the first, second and third rows [colored in pink, yellow and cyan in panel **(A)**, respectively] of IHC from control heterozygous (black, gray) or homozygous *shaker2* (dark and light blue) littermates cultured in control conditions (darker points) or with tubocurarine (lighter points). Horizontal lines indicate the mean and statistical differences were obtained using Welch's *t* tests. **(D)** Representative focused ion beam SEM (FIB-SEM) images from homozygous *shaker2* mice cultured at 37°C in control conditions for 4 h (*top*), with 60 µM tubocurarine for 5.5 h (*middle*), or with 300 µM tubocurarine for 4 h (*bottom*). **(E)** Heights of stereocilia from the first and second rows of the bundle obtained from FIB-SEM images of homozygous *shaker2* IHC cultured in control conditions (darker points) or with tubocurarine (lighter points). Horizontal lines indicate the mean and statistical differences were obtained using a Šídák's multiple comparisons test. For all panels, the age of explants is P5, and statistical significance is shown as: *$p < 0.05$, **$p < 0.01$, ***$p < 0.001$, ****$p < 0.0001$; n.s., not significant.

The entry of FM1-43 dye through MET channels open at rest was significantly blocked by tubocurarine in IHC and OHC of homozygous mice lacking the long isoform of MYO15A and their heterozygous and wild-type littermates (Figure 3A), indicating the presence of resting MET currents in all three genotypes. We next exposed neonate organ of Corti explants to MET channel blockers and measured changes to the stereocilia morphology by using SEM. In explants cultured in control conditions for 4 h, mice lacking one (heterozygous *Myo15a*$^{+/\Delta N}$) or two (homozygous *Myo15a*$^{\Delta N/\Delta N}$) alleles of the long isoform of MYO15A exhibited stereocilia bundle staircase arrangements similar to those observed in wild-type littermates (Figures 3B, 4A). For OHC, the diameters of second row stereocilia were indistinguishable between all three genotypes (Supplementary Figures 5A,B) and so were the heights (comparisons against wild-type littermates: $p = 0.1178$ for heterozygous and $p = 0.9156$ for homozygous mice). For IHC, however, second row stereocilia exhibited similar heights in all three genotypes (comparisons against wild-type littermates: $p = 0.2774$ for heterozygous and $p = 0.2527$ for homozygous mice) but the tip diameters were significantly smaller in mice lacking one or two alleles of the long isoform of MYO15A (Supplementary Figures 5C,D).

As expected in wild-type mice, a 4-h incubation with the MET channel blocker tubocurarine (300 µM) led to significant thinning of the second row stereocilia in OHC and IHC bundles (Figures 3B,C, 4A,B) but no significant shortening of transducing second and third row stereocilia (Figures 3D, 4C). In contrast, homozygous mice lacking the long isoform of MYO15A (*Myo15a*$^{\Delta N/\Delta N}$) showed significant shortening of transducing second and third row stereocilia, beyond the initial phase of stereocilia thinning

10.3389/fneur.2024.1482892

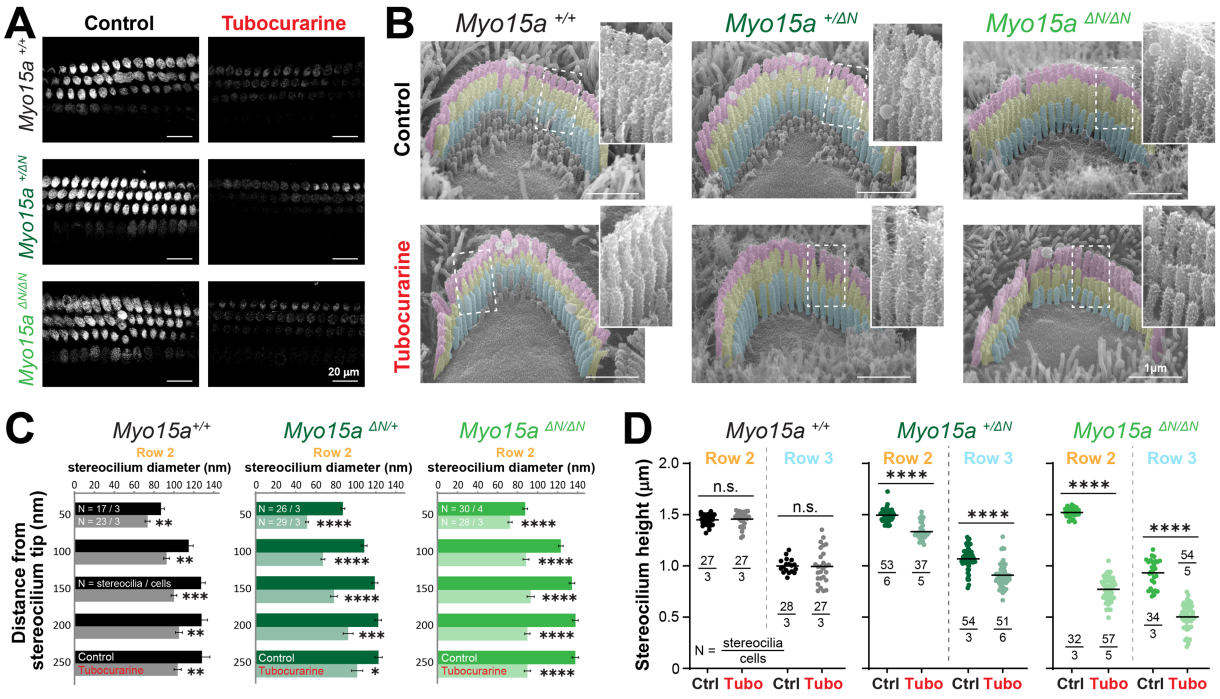

FIGURE 3
Outer hair cells lacking the long isoform of MYO15A show accelerated mechanotransduction-dependent stereocilia remodeling. **(A)** Decreased FM1-43 dye uptake in hair cells after application of the MET channel blocker, tubocurarine (300 µM), in wild-type *Myo15a*$^{+/+}$ (*top*), heterozygous *Myo15a*$^{+/\Delta N}$ (*middle*) or homozygous *Myo15a*$^{\Delta N/\Delta N}$ (*bottom*) littermates. **(B)** Representative false-colored SEM images of OHC stereocilia bundles cultured for 4 h at 37°C in control conditions (*top*) or with 300 µM tubocurarine (*bottom*), from wild-type (*left*), heterozygous mice (*middle*) or homozygous *Myo15a*$^{\Delta N}$ (*right*) littermates. Insets show highlighted bundle regions at higher magnification. **(C)** Diameter of stereocilia from the second row [colored in yellow in panel **(B)**] at several positions from the stereocilium tip from OHC of wild-type (black), heterozygous (darker shades of green) and homozygous *Myo15a*$^{\Delta N}$ (brighter shades of green) littermates cultured in control conditions (darker bars) or with tubocurarine (lighter bars). Data are shown as mean ± SE. Statistical differences were analyzed using a linear mixed model. **(D)** Stereocilia heights from the second and third rows [colored in yellow and cyan, respectively, in panel **(B)**] of OHC from control wild-type (black, gray), heterozygous (darker shades of green) or homozygous *Myo15a*$^{\Delta N}$ (brighter shades of green) littermates cultured in control conditions (darker points) or with tubocurarine (lighter points). Horizontal lines indicate the mean and statistical differences were obtained using a Šídák's multiple comparisons test. For all panels, the age of explants is P7, and statistical significance is shown as: *$p < 0.01$, **$p < 0.001$, ***$p < 0.001$, ****$p < 0.0001$; n.s., not significant. Data are representative of four independent series with 3–4 h incubations with 300 µM tubocurarine in P4–P7 explants.

(Figures 3B,D, 4A,C; Supplementary Figures 5B,D). Mice lacking just one allele of the long isoform of MYO15A (*Myo15a*$^{+/\Delta N}$) showed an intermediate response to MET channel blockage between wild-type and homozygous littermates (Supplementary Figures 5B,D) with significant thinning in the tips of second row stereocilia (Figures 3B,C, 4A,B) as well as significant stereocilia shortening (Figures 3D, 4C). These results were surprising given that mice lacking just one allele of the long isoform of MYO15A appear to have normal hearing (26).

Similar results were obtained after a longer incubation period (24 h) with benzamil, a MET channel blocker pharmacologically unrelated to tubocurarine, at a 30 µM concentration which was shown to block ~90% of MET currents induced by bundle deflections (28). MET channel blockage led to significant shortening of transducing stereocilia in IHC and OHC from heterozygous and homozygous *Myo15a*$^{\Delta N}$ mice and, once again, the degree of stereocilia shortening was significantly greater in the homozygous mice (Supplementary Figure 6).

Altogether, these results indicate that the long isoform of MYO15A (MYO15A-1) delivers molecular machinery to the tips of transducing stereocilia crucial for proper cytoskeleton stability to avoid exaggerated MET-dependent stereocilia remodeling.

2.3 Stereocilia in the tallest row of the hair bundle exhibit MET-dependent remodeling when the long isoform of MYO15A is absent

The heights of stereocilia from the tallest row were shorter in mice lacking one or two alleles of the long isoform of MYO15A in OHC (Figure 5A, comparisons against wild-type littermates: $p = 0.02$ for heterozygous and $p < 0.0001$ for homozygous mice) and IHC (Figure 5C, comparisons against wild-type littermates: $p = 0.04$ for heterozygous and $p = 0.008$ for homozygous mice). In our previous study (11), we showed that the MET-dependent remodeling of stereocilia was limited to the transducing rows of the bundle. Consistent with our previous study, no changes in stereocilia heights were observed in wild-type OHC or IHC cells after MET channel blockage with 300 µM of tubocurarine for 4 h (Figures 5A,C). To our surprise, careful examination of stereocilia bundle dimensions in our SEM images revealed significant shortening of stereocilia in the tallest row of IHC and OHC bundles in mice lacking one or both alleles of the long isoform of MYO15A (Figures 5A,C and Supplementary Figure 7). This MET-induced

10.3389/fneur.2024.1482892

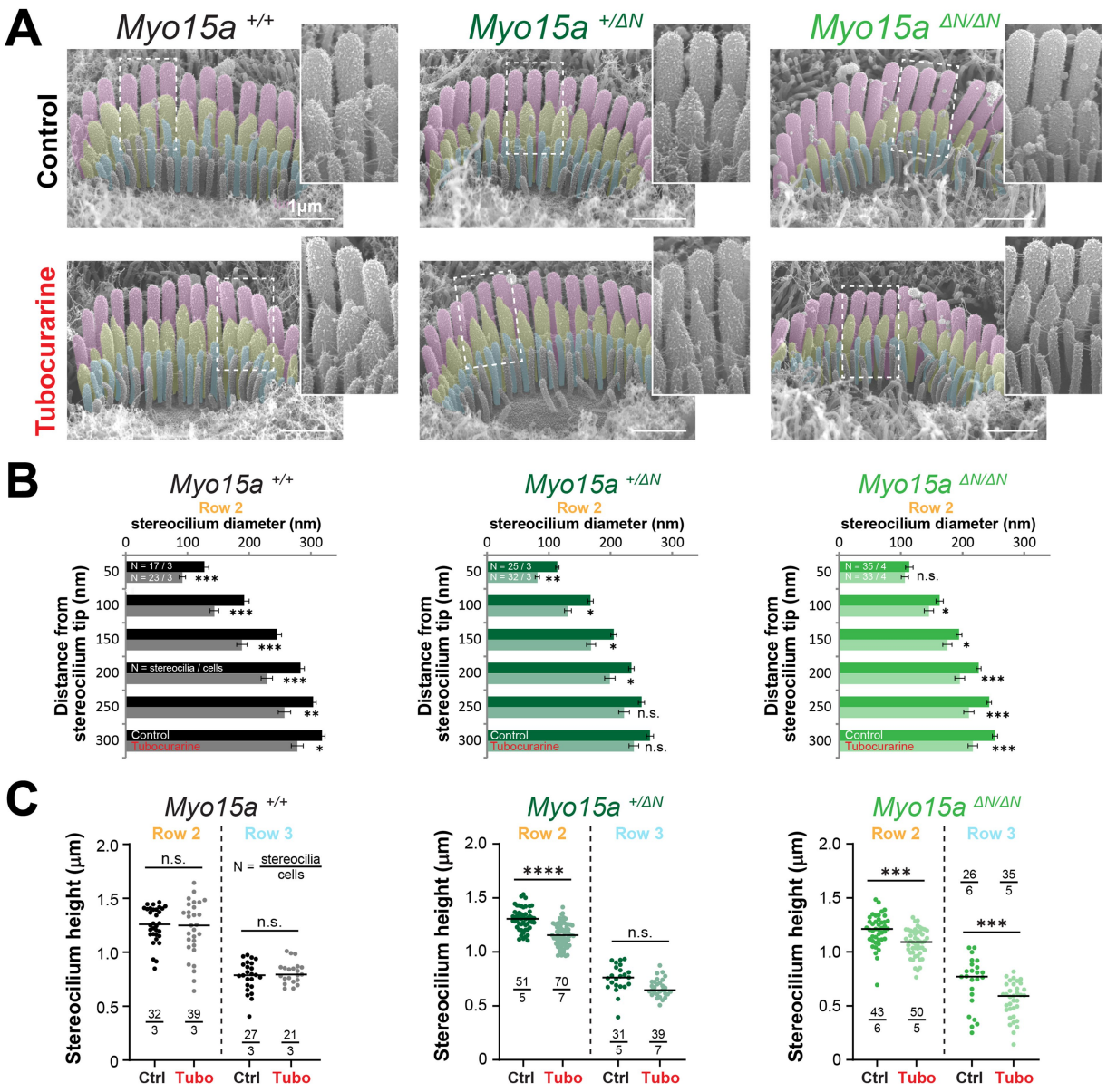

FIGURE 4
Inner hair cells lacking the long isoform of MYO15A show accelerated MET-dependent stereocilia remodeling. **(A)** Representative SEM images of IHC stereocilia bundles from wild-type (*left*), heterozygous (*middle*), or homozygous *Myo15a*$^{\Delta N}$ (*right*) littermates cultured for 4 h at 37°C in control conditions (*top*) or with 300 µM tubocurarine (*bottom*). Insets show highlighted bundle regions at higher magnification. **(B)** Diameter of stereocilia from the second row of IHC [colored in yellow in panel **(A)**] at several positions from the stereocilium tip, from wild-type (black), heterozygous (dark shades of green), and homozygous *Myo15a*$^{\Delta N}$ (bright shades of green) littermates cultured in control conditions (darker bars) or with tubocurarine (lighter bars). Data are shown as mean ± SE. Statistical differences were analyzed using a linear mixed model. **(C)** Stereocilia heights from the second and third row of IHC [colored in yellow and cyan, respectively, in panel **(A)**] from wild-type (black), heterozygous (darker shades of green), or homozygous *Myo15a*$^{\Delta N}$ (brighter shades of green) littermates cultured in control conditions (darker points) or with tubocurarine (lighter points). Horizontal lines indicate the mean and statistical differences were obtained using Šídák's multiple comparisons test. For all panels, the age of explants is P7, and statistical significance is shown as: *$p < 0.01$, **$p < 0.001$, ***$p < 0.001$, ***$p < 0.0001$; n.s., not significant. Data are representative of four independent series with 3–4 h incubations with 300 µM tubocurarine in P4–P7 explants.

shortening of stereocilia from the tallest row of the bundle lacked the typical initial step of stereocilia tip thinning seen in transducing stereocilia (Figures 3B, 4A and Supplementary Figure 7). We did observe some small differences in the diameters of tallest row stereocilia from mice lacking one or both alleles of the long isoform of MYO15A, but these stereocilia tip diameters were largely maintained after MET channel blockage (Figures 5B,D). MET channel blockage with 30 µM of benzamil for 24 h also showed significant shortening of IHC and OHC stereocilia from the tallest row of the bundle in heterozygous and homozygous *Myo15a*$^{\Delta N}$ littermates (Supplementary Figure 6).

To confirm the shortening of row 1 stereocilia that was triggered by MET channel blockage, we performed fluorescent labeling of F-actin and high-resolution confocal microscopy in mice lacking one

10.3389/fneur.2024.1482892

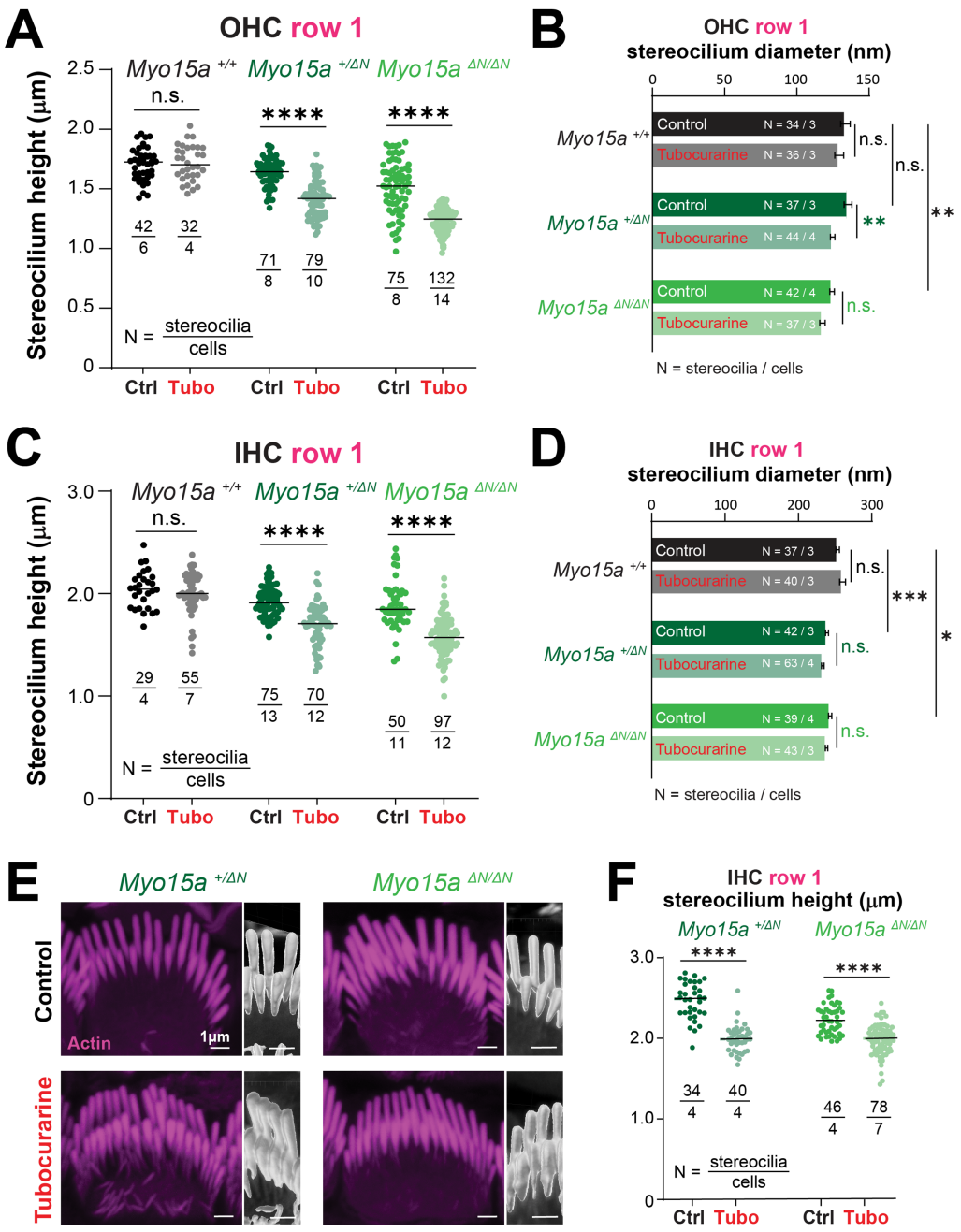

FIGURE 5
Hair cells lacking the long isoform of MYO15A exhibit MET-dependent stereocilia remodeling in the tallest row of the bundle. **(A–D)** Stereocilia heights **(A,C)** and diameters **(B,D)** from the first row of OHC **(A,B)** and IHC **(C,D)** from wild-type (black and gray), heterozygous (darker shades of green) or homozygous *Myo15a*$^{\Delta N}$ (brighter shades of green) littermates that were cultured in control conditions (darker points/bars) or with 300 µM tubocurarine (lighter points/bars) for 4 h at 37°C. Data are representative of four independent series with 3–4 h incubations with 300 µM tubocurarine in P4–P7 explants. **(E)** Confocal images of IHC stereocilia stained against F-actin with fluorescently-labeled phalloidin (magenta), cultured for 4 h at 37°C in control conditions (*top*) or with 300 µM tubocurarine (*bottom*), from heterozygous (*left*) and homozygous *Myo15a*$^{\Delta N}$ (*right*) littermates. Insets show bundle regions with Imaris volume render at higher magnification. Images are representative of two independent experiments. **(F)** Stereocilia heights from the first row of IHC from heterozygous (dark shades of green) or homozygous *Myo15a*$^{\Delta N}$ (bright shades of green) littermates cultured in control conditions (darker points) or with tubocurarine (lighter points). Stereocilia heights were measured from Imaris volume rendering of the confocal stacks. For all panels, the age of explants is P7, and statistical significance is shown as: *$p < 0.01$, **$p < 0.001$, ***$p < 0.001$, ****$p < 0.0001$; n.s., not significant. In panels **(B)** and **(D)**, significant differences are shown for control conditions between genotypes (black, relative to wild-type), or between control and tubocurarine conditions within each genotype (color coded for each genotype: black for wild-type, dark green for heterozygous, and bright green for homozygous *Myo15a*$^{\Delta N}$ littermates).

or both alleles of the long isoform of MYO15A cultured with 300 µM of tubocurarine for 4 h. Volume rendering of the confocal stacks once again revealed a significant MET-induced decrease in the heights of stereocilia from the tallest row of IHC from heterozygous and homozygous mice lacking the long isoform of MYO15A (Figures 5E,F).

We conclude that the absence of the long isoform of MYO15A results in decreased stability of the actin cytoskeleton within stereocilia from the tallest row of the bundle.

2.4 The absence of the long isoform of MYO15A leads to the mislocalization of several row identity proteins

Since the long isoform of MYO15A typically accumulates at the tips of transducing stereocilia, we were surprised to observe MET-induced changes to the morphology of stereocilia in the tallest row of the bundle from mice lacking MYO15A-1. Therefore, we wondered whether the 'row identity' of stereocilia was affected. To test this, we performed immunolabeling against some known proteins that show preferential expression in the tips of stereocilia from either the tallest row or the transducing rows.

First, we evaluated the expression of ESPNL, a protein with high similarity to the crosslinker ESPN, predicted to have only one actin-binding domain, and detected during hair bundle development (up to ~P11) as highly enriched in transducing stereocilia (31). As expected, in wild-type IHC we observed labeling of ESPNL that was enriched in the transducing stereocilia at the two different developmental ages and two cochlear regions tested: apical and middle regions, at P3 (Figure 6A) and P7 (Figure 6B). However, the ESPNL labeling in homozygous *Myo15a*$^{\Delta N/\Delta N}$ IHC first appeared rather diffuse throughout the entire bundle (Figure 6A) and was no longer detected by P7 (Figure 6B). IHC from heterozygous *Myo15a*$^{+/\Delta N}$ mice exhibited intermediate labeling patterns to those observed in wild-type and homozygous littermates (Figure 6).

Next, we evaluated whether proteins from the row 1 elongation complex were affected in mice lacking the long isoform of MYO15A. As described previously (26), the expression pattern of the actin capping/bundling protein EPS8 appears to be unaffected by the lack of MYO15A-1: it remains highly expressed at the tips of stereocilia from the tallest row in IHC and OHC from homozygous and heterozygous *Myo15a*$^{\Delta N}$ mice, similar to what is observed in wild-type mice (Figures 7A,B). At the time the *Myo15a*$^{\Delta N}$ mice were first characterized, the role of the GPSM2-GNAI3 signaling complex in stereocilia elongation had not been reported. Thus, we next evaluated the expression pattern of GNAI3 in hair cells from mice lacking one or both alleles of MYO15A-1 and in wild-type mice. While GNAI3 was still preferentially trafficked to the tips of stereocilia in the tallest row of the bundle, we noticed several stereocilia that lacked GNAI3 labeling in OHC from heterozygous and homozygous *Myo15a*$^{\Delta N}$ mice (Figure 7C), while the GNAI3 labeling in IHC appeared normal (Figure 7D). The GPSM2-GNAI3 signaling complex is also highly expressed in the "bare zone" of hair cells—the apical region of hair cells near the kinocilium that is deprived of stereocilia during the hair bundle development—where it contributes to proper establishment of planar cell polarity (18), and we found similar GNAI3 labeling of the bare zone region in hair cells from mice lacking one or both alleles of MYO15A-1 as in wild-type mice (Supplementary Figure 8).

Our results indicate that, in the absence of the long isoform of MYO15A, several row identity proteins might not be trafficked properly.

3 Discussion

Our study is the first to show that MYO15A isoforms are necessary for the MET-dependent remodeling of the stereocilium actin cytoskeleton. We focused on the MET-driven plasticity of the stereocilium cytoskeleton of hair cells from the middle region of the mouse cochlea after postnatal day 4, once the initial stages of stereocilia elongation and thickening are completed and when row identity within the bundle has been clearly established. Under these conditions, the MET-dependent remodeling of the actin cytoskeleton is limited to the transducing shorter rows of stereocilia while stereocilia from the tallest row remains unaffected (11, 12).

3.1 Which MYO15A isoform delivers the molecular machinery that allows for MET-dependent stereocilia remodeling?

We did not observe any evidence of MET-dependent stereocilia remodeling in hair cells from *shaker-2* mice in which all isoforms of MYO15A are nonfunctional. Although we cannot completely rule out that remodeling could still happen in specific conditions not tested here, it is tempting to speculate that MYO15A isoforms either deliver (*i*) all molecular machinery required for the MET-driven remodeling of the stereocilium cytoskeleton, or (*ii*) machinery that works in series with proteins delivered by other myosin motors. In contrast, the absence of the long isoform of MYO15A (MYO15A-1) led to exaggerated MET-dependent stereocilia remodeling in the shorter rows and to unexpected remodeling in the tallest row. These findings indicate that MYO15A-2 and/or MYO15A-3 likely deliver the molecular machinery that enables stereocilia cytoskeleton rearrangements in response to changes in the resting MET current. However, at this point we cannot speculate on the specific MYO15A isoform that delivers such machinery because the expression levels and bundle localization of MYO15A-3 are still unknown. Nonetheless, this study highlights the need to explore whether MYO15A-3 is involved in the MET-driven remodeling of the stereocilium cytoskeleton using mice deficient in this isoform.

3.2 MYO15A-1 delivers machinery that increases the stability of the stereocilium actin cytoskeleton

While the MET-dependent remodeling of stereocilia was present in the absence of MYO15A-1, this remodeling appeared to occur at a significantly faster rate. Therefore, MYO15A-1 likely delivers molecular machinery that increases the cytoskeleton stability during the MET-driven remodeling of the stereocilium cytoskeleton. Since this isoform is preferentially trafficked to the shorter rows of the bundle, it was not surprising to observe changes in the degree of MET-dependent remodeling in the transducing stereocilia. In fact, shifting the balance toward greater MET-dependent stereocilium remodeling by decreasing the stability of the stereocilium cytoskeleton could also explain why mice deficient in MYO15A-1 exhibit premature stereocilia degeneration and subsequent hearing loss (26). MYO15A-1 is also trafficked to the tips of row 1 stereocilia in OHC (26), which could explain the unexpected MET-dependent remodeling that

10.3389/fneur.2024.1482892

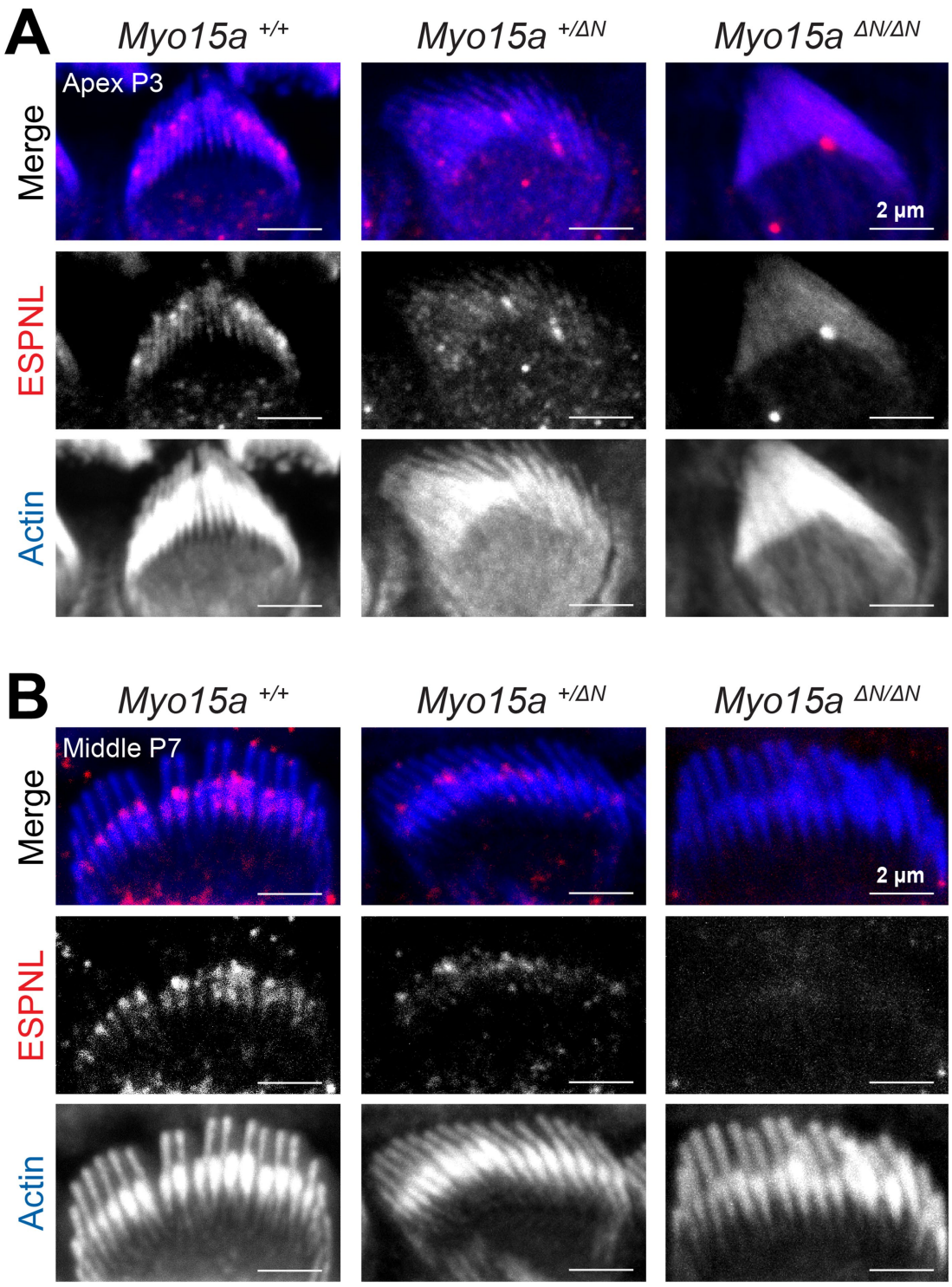

FIGURE 6
Impaired expression of ESPNL in inner hair cells lacking the long isoform of MYO15A. Maximum intensity projections of confocal stacks of IHC stereocilia from the apical **(A)** or middle **(B)** cochlear regions, at postnatal days 3 **(A)** or 7 **(B)**, from wild-type (*left*), heterozygous (*middle*), and homozygous *Myo15a*$^{\Delta N}$ (*right*) mice immunolabeled against ESPNL (red) and counterstained against F-actin with fluorescently-labeled phalloidin (blue). Images are representative of two independent experiments, with similar labeling patterns along different cochlear regions.

we observed in stereocilia from the tallest row in OHC. However, this hypothesis would not explain the MET-dependent remodeling that we observed in row 1 stereocilia from IHC (which normally lack MYO15A-1).

The exact molecular machinery delivered by MYO15A isoforms to allow and fine-tune the extent of MET-dependent remodeling in the stereocilium cytoskeleton remains to be fully explored. It is plausible that the lack of expression of MYO15A-1 affects the normal

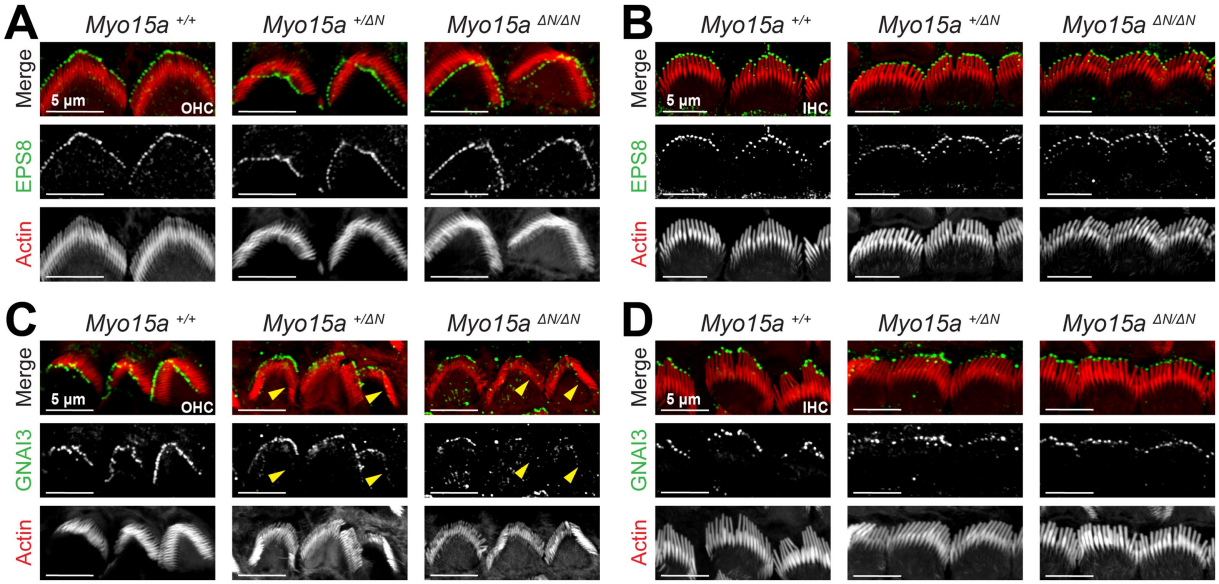

FIGURE 7
GNAI3 is mislocalized in outer, but not inner, hair cells lacking the long isoform of MYO15A. Maximum intensity projections of confocal stacks of OHC **(A,C)** and IHC **(B,D)** stereocilia from wild-type (*left*), heterozygous (*middle*), and homozygous *Myo15a*$^{\Delta N}$ (*right*) mice immunolabeled against EPS8 (green) **(A,B)** or GNAI3 **(C,D)**, and counterstained against F-actin with fluorescently-labeled phalloidin (red). Yellow arrowheads point to OHC regions lacking GNAI3 labeling in heterozygous and homozygous *Myo15a*$^{\Delta N}$ mice. In panels **(C)** and **(D)**, the maximum intensity projections ignored Z planes near the cuticular plate to avoid confounding GNAI3 labeling from the bare zone of hair cells. Images are representative of two independent experiments. To see the GNAI3 labeling in the bare zone, see Supplementary Figure 8. In all panels the age of explants is P7.

expression levels and/or distribution of MYO15A-3 within the bundle, which remains to be tested. Additionally, we observed a decrease in the expression of ESPNL in transducing stereocilia from mice lacking one or two alleles of MYO15A-1. Although ESPNL is a known cargo protein of MYO3A (31), its expression is still present at the tips of stereocilia from hair cells lacking both MYO3A and MYO3B (32). However, it remains to be explored whether ESPNL could be a cargo of MYO15A. Given the increased levels of MET-dependent remodeling in transducing stereocilia from mice lacking MYO15A-1, perhaps ESPNL is required to increase the stability of the stereocilium actin cytoskeleton. In support of this hypothesis, mice lacking ESPNL show degeneration of transducing stereocilia (31).

3.3 Are MET channels present in row 1 stereocilia in the absence of MYO15A-1?

Another hypothesis explaining the MET-dependent remodeling of stereocilia within the tallest row of the bundle in the absence of MYO15A-1 is that, perhaps, some MET channels are mislocalized to the upper end of the tip link. In this scenario, stereocilia from the tallest row would also experience a resting MET current. Since the MET-driven shortening of stereocilia in the tallest row is rather uniform, it would indicate that all stereocilia within the tallest row have MET channels at the upper tip link end. Thus, could hair cells lacking the long isoform of MYO15A possibly have larger MET currents upon bundle deflections? Previously, abnormal current-displacement MET curves were described for *Myo15a*$^{\Delta N/\Delta N}$ mice relative to their *Myo15a*$^{+/\Delta N}$ littermates (26). Larger maximum MET currents were indeed reported for OHC (and perhaps IHC at larger displacements) in *Myo15a*$^{+/\Delta N}$ mice. However, that study did not evaluate wild-type littermates. In addition, MET currents were assessed with a stiff probe, which did not allow for proper measurements of resting MET currents. Therefore, the presence of abnormal resting MET currents cannot be ruled out in mice lacking one or two alleles of MYO15A-1.

3.4 Is the lack of MYO15A-1 altering the normal stages of hair bundle development?

MET-driven rearrangements of the actin cytoskeleton in stereocilia from the tallest row have been observed at early developmental bundle stages [e.g., at P4 in apical hair cells in Krey et al. (12)]. Heterozygous *Myo15a*$^{+/\Delta N}$ mice develop normal hearing, yet they exhibited an intermediate MET-dependent stereocilia remodeling phenotype, including remodeling of stereocilia from the tallest row. Therefore, it is possible that the lack of one or two alleles encoding MYO15A-1 slightly alters the normal developmental stages of the hair bundle. In this case, the differences in MET-dependent stereocilium remodeling that we observed in this study could simply be the result of comparisons between cells in slightly different developmental stages. Consistent with this hypothesis, we did observe significant differences in stereocilia diameters from the tallest and middle rows of IHC bundles and in the heights of IHC and OHC stereocilia from the tallest row between mice lacking one or two alleles of MYO15A-1 and their wild-type littermates (Figures 5A–D; Supplementary Figure 5C).

Due to this unexpected MET-driven remodeling in stereocilia from the tallest row, we also explored the expression levels of GNA13, a 'row-identity' signaling protein trafficked to the tips of stereocilia from row 1. GNAI3 is detected in some stereocilia tips by E18.5 and virtually in all row 1 stereocilia tips by P4 (18). In mice lacking one or two copies of MYO15A-1, however, GNAI3 labeling was still lacking

in several OHC stereocilia tips by P7. Once again, these results could be consistent with defects in the proper stages of bundle development and the establishment of stereocilium row identity within the bundle of these mutant mice. Alternatively, the GPSM2-GNAI3 signaling complex might be crucial for the normal stability of the actin cytoskeleton in stereocilia from the tallest row of the bundle and their insensitivity to changes in resting MET current levels.

3.5 Could haploinsufficiency of MYO15A-1 increase susceptibility to hearing loss?

Adult heterozygous *Myo15a*$^{+/\Delta N}$ mice might have a hidden hearing phenotype. Perhaps the larger extent of MET-driven stereocilium remodeling in these mice works near a normal physiological range. However, under certain conditions—such as the noise-induced breakage of tip links—, the larger MET-dependent remodeling of transducing stereocilia could lead to some stereocilia degeneration. Therefore, we believe it is worth exploring whether *Myo15a*$^{+/\Delta N}$ mice are more susceptible to noise-induced or age-related hearing loss than their wild-type littermates.

3.6 Distinct morphological changes of MET-dependent remodeling between stereocilia rows

An additional interesting observation regarding the MET-dependent remodeling of stereocilia from the tallest row was the lack of stereocilia thinning at the tips, like we typically observe in stereocilia from the shorter rows of the bundle. In the presence of tip links, the MET-dependent remodeling of transducing stereocilia starts with significant thinning of stereocilia tips and eventual shortening. Previously, we only observed uniform shortening of transducing stereocilia (not preceded by stereocilium tip thinning) after tip link breakage with BAPTA-buffered extracellular medium (11). We hypothesized that the thinning at the stereocilium tip was due to the partial blockage (~70–90%) of MET channels. We thought a small influx of calcium ions was able to stabilize actin filaments near the MET channel while actin filaments at the periphery of the stereocilium—far from the MET channel and experiencing low intracellular calcium concentrations—would depolymerize first. Here, we used a saturating concentration of MET channel blocker, yet we still observed significant thinning at the stereocilium tips instead of uniform stereocilium shortening. These results likely indicate the presence of additional signaling pathways provided by the tip links that help stabilize the stereocilium actin cytoskeleton. In support of this hypothesis, a recent study shows that tip-link mutant mice exhibit some differences in stereocilia bundle dimensions that cannot solely be explained by defects in MET currents (13).

4 Methods

4.1 Mice and cochlear explants

Organ of Corti explants from *Myo15*$^{sh2/sh2}$, *Myo15*$^{\Delta N/\Delta N}$, *CIB2*$^{F91S/F91S}$ and *CIB2*$^{tm1a/\ tm1a}$ mice along with their heterozygous and wild-type littermates were isolated at postnatal days 4 through 7. *Myo15*$^{sh2/sh2}$ mice are maintained in the laboratory in an inbred mixed background (B6N-Tyr$^{c\text{-}Brd}$/BrdCrCrl and C57Bl/6 J). *Myo15*$^{\Delta N/\Delta N}$ mice generated by Dr. Jonathan Bird (26) are maintained in a B57Bl/6 background. *CIB2*$^{F91S/F91S}$ and *CIB2*$^{tm1a/tm1a}$ mice generated by Dr. Zubair Ahmed (30) and maintained in a B57Bl/6J background were kindly provided to us by Dr. Gregory Frolenkov. Temporal bones from the mice were isolated, and access to the cochlea was gained by removing surrounding bone. Following the bone removal, the modiolus and stria vascularis were subsequently removed. The cochlear explants were held in place during incubations and live-cell imaging by two flexible glass fibers glued to the bottom of a plastic Petri dish.

The University of Kentucky Institutional Animal Care and Use Committee granted approval for all animal procedures (protocol 2020-3535 to A.C.V.)

4.2 Incubations with MET channel pharmacological blockers

Organ of Corti explants were cultured in DMEM (Gibco, 11-995-065) supplemented with 7% FBS (Gibco, 16140071) and 10 mg/mL ampicillin (Calbiochem, 171254), at 37°C and 5% CO_2 for up to 24 h with 30 μM of benzamil (Sigma, B2417) in DMSO (VWR, N182-5X), with 60 or 300 μM of tubocurarine (Sigma Aldrich, 93750), 20 μM of BAPTA-AM (Invitrogen, B6769) pre-mixed with 20% Pluronic F-127 solution in DMSO (Invitrogen, P3000MP), or in vehicle-control conditions (0.05% DMSO). All samples had their tectorial membrane removed after incubation and were fixed in either 4% paraformaldehyde (PFA) (for subsequent immunolabeling), formaldehyde/glutaraldehyde (3% each) in 0.1 M sodium cacodylate buffer (Electron Microscopy Sciences, 15950) supplemented with 2 mM of $CaCl_2$ (Sigma-Aldrich, 16538-06) (for scanning electron microscopy) or 2% PFA/2.5% glutaraldehyde in 0.1 M sodium cacodylate buffer (Electron Microscopy Sciences, 15960-01) with 1% tannic acid (Sigma Aldrich, 403040) (for focused ion beam electron microscopy).

4.3 FM1-43 dye uptake

Freshly-isolated organ of Corti explants were incubated for 30 s with cold Ca^{2+}/Mg^{2+}-free Hank's balanced salt solution (HBSS) (Gibco, 14175-079) supplemented with 5 μM of FM1-43 dye (ThermoFisher, T35356) in the absence or presence of the MET channel blocker tubocurarine. The explants were rinsed several times with cold Leibovitz's L-15 (Gibco, 21-083-027) and imaged immediately. Images were acquired using a Leica SP8 upright confocal microscope equipped with a Leica XCX APO L 63X 0.9 NA water immersion objective.

4.4 Immunolabeling and confocal microscopy

All samples were fixed with cold 4% PFA supplemented with 20 mM $CaCl_2$. Samples were in the fixative solution at least 24 h at 4°C. Samples then were rinsed in PBS (Gibco, 10010023) and then

permeabilized in 0.5% Triton™ X-100 (Electron Microscopy Sciences, 22142) in PBS for 1 h. Samples were next blocked for 2 h with a solution of 5% normal goat serum (Invitrogen, 10000c), 2% bovine serum albumin (BSA, Thermofisher scientific, 37525) and 0.25% Triton™ X-100. Samples were incubated overnight with primary antibodies against EPS8 (BD Biosciences, 610143, at 1:100), GNAI3 (Millipore Sigma, G4040, at 1:100), or ESPNL (at 1:50, previously characterized in Ebrahim et al. (31)) at 4°C. Samples were rinsed with PBS and 0.2% BSA and incubated with fluorescently labeled secondary antibodies (Alexa Fluor 555 goat anti-mouse, ThermoFisher Scientific, A-21127, at 1:100; *CF* 555 goat anti-rabbit, Sigma-Aldrich, SAB4600068, at 1:100; or Alexa Fluor 488 goat anti-rabbit, ThermoFisher Scientific, A-11034, at 1:1,000) for 3 h at 120 rpm at room temperature. The samples were counterstained at room temperature with either rhodamine phalloidin (1 unit, ThermoFisher Scientific, R415) for 30 min or Alexa Fluor 488 phalloidin (1 unit, ThermoFisher Scientific, A12379) for 45 min. Tissues were rinsed in PBS, mounted in ProLong Diamond antifade (ThermoFisher Scientific, P36965) and allowed to cure for 72 h before imaging. Images were acquired from the middle cochlear region with a Leica SP8 upright confocal microscope equipped with a Leica HCX PL APO 100X 1.44 NA objective lens. The typical voxel size used during imaging acquisition of hair cell bundles was ~20 nm in X and Y, and 50 nm in Z. Imaging drifts were corrected in Huygens software.

4.5 Scanning electron microscopy (SEM)

Organ of Corti explants were fixed in cold formaldehyde/glutaraldehyde (3% each) in 0.1 M sodium cacodylate buffer supplemented with 2 mM of $CaCl_2$ as described above. Samples were kept in fixative at 4°C for at least 24 h until further processing. Distilled water was used to rinse the samples, followed by dehydration through a graded series of ethanol (VWR, 89125-170). Subsequently, samples were subjected to critical point drying from liquid CO_2 (Leica, CPD300) and coated with 5 nm platinum through sputter coating (Quorum Technologies, Q150T). Hair cells from the middle cochlear region (near the 50% point in cochlear length) were imaged with a field-emission scanning electron microscope (FEI, Helios Nanolab 660). This work was performed in part at the U.K. Electron Microscopy Center, a member of the National Nanotechnology Coordinated Infrastructure (NNCI), which is supported by the National Science Foundation (NNCI-2025075).

For accurate stereocilia height measuring, images of the same bundle were obtained from different angles, including views from the lateral (back) and medial (front) sides of the bundle. Measurements were performed on Fiji ImageJ. Calculations of the heights of each stereocilium were performed as described in Velez-Ortega et al. (11).

4.6 Focused ion beam scanning electron microscopy (FIB-SEM)

Organ of Corti explants were fixed in 2% PFA/2.5% glutaraldehyde in 0.1 M sodium cacodylate buffer (Electron Microscopy Sciences, 15960-01) supplemented in 1% tannic acid (Sigma Aldrich, 403040). Distilled water was used to rinse the samples, followed by a graded series of glycerol (Electron Microscopy Sciences, 16550). Samples underwent plunge freezing using liquid nitrogen. Samples were then moved to a 1:1 solution of liquid nitrogen and 1% uranium acetate (Electron Microscopy Sciences, 22400) before undergoing freeze substitution and low temperature embedding (Leica, EMAFS2) with graded series of methanol (Electron Microscopy Sciences, 18511), lowicryl (Electron Microscopy Sciences, 14330) and curing with UV light. Resin blocks were thinned (Leica, SM2000R), trimmed (Boeckeler Instruments, PTXLPowerTome) and coated with 25 nm platinum through sputter coating (Quorum Technologies, Q150T). Samples were then milled with a focused ion beam (65 nA) at 20 nm steps and imaged (near the mid-point of the cochlea) with a field-emission scanning electron microscope (FEI, Helios Nanolab 660) at the U.K. Electron Microscopy Center.

4.7 Statistical analysis

Data is shown as Mean ± SE, unless otherwise noted. Asterisks denote statistical significance from either Welch's *t* tests, Mann–Whitney tests, Šídák's multiple comparisons tests, or linear mixed effect models using Prism (GraphPad Software) or Origin (OriginLab Corp.). Results are shown with *p* values <0.05 (*), <0.01 (**), <0.001 (***) or <0.0001 (****) and the specific test is indicated in each figure legend.

5 Conclusion

Altogether, our results indicate that MYO15A isoforms deliver to the tips of shorter stereocilia molecular machinery required to allow the remodeling of the actin cytoskeleton in response to changes in resting MET currents. In addition, MYO15A-1 specifically delivers machinery to increase cytoskeleton stability—thus preventing exaggerated MET-dependent stereocilium remodeling—and influences the row identity of stereocilia.

Data availability statement

The raw data supporting the conclusions of this article will be made available by the authors without undue reservation.

Ethics statement

The animal study was approved by University of Kentucky Institutional Animal Care and Use Committee. The study was conducted in accordance with the local legislation and institutional requirements.

Author contributions

AL-P: Data curation, Formal analysis, Investigation, Methodology, Visualization, Writing – original draft. AK: Investigation, Methodology, Visualization, Writing – review & editing. MM: Investigation, Methodology, Writing – review & editing. AV-O: Conceptualization, Data curation, Funding acquisition, Project

administration, Supervision, Visualization, Writing – original draft, Writing – review & editing.

Funding

The author(s) declare that financial support was received for the research, authorship, and/or publication of this article. This work was supported by the NIH/NIDCD R01DC021325 and R21DC017247 to A.C.V.

Acknowledgments

The authors would like to thank Dr. Peter Barr-Gillespie for providing ESPNL antibodies; Drs. Zubair Ahmed and Gregory Frolenkov for providing the mechanotransduction-deficient (*Cib2* mutant) mice; Dr. Basile Tarchini for suggestions on antibodies against GNAI3 and GPSM2; Drs. Jonathan Bird and Gregory Frolenkov for helpful discussions and comments throughout the execution of this study; and miss Abigail Dragich for her constructive comments on the manuscript draft. This article was submitted as a preprint to BioRxiv as López-Porras et al. (33).

Conflict of interest

The authors declare that the research was conducted in the absence of any commercial or financial relationships that could be construed as a potential conflict of interest.

Publisher's note

Supplementary material

The Supplementary material for this article can be found online at: https://www.frontiersin.org/articles/10.3389/fneur.2024.1482892/full#supplementary-material

References

1. Shin JB, Longo-Guess CM, Gagnon LH, Saylor KW, Dumont RA, Spinelli KJ, et al. The R109H variant of fascin-2, a developmentally regulated actin crosslinker in hair-cell stereocilia, underlies early-onset hearing loss of dba/2J mice. *J Neurosci*. (2010) 30:9683–94. doi: 10.1523/JNEUROSCI.1541-10.2010

2. Taylor R, Bullen A, Johnson SL, Grimm-Gunter EM, Rivero F, Marcotti W, et al. Absence of plastin 1 causes abnormal maintenance of hair cell stereocilia and a moderate form of hearing loss in mice. *Hum Mol Genet*. (2015) 24:37–49. doi: 10.1093/hmg/ddu417

3. Tilney LG, Derosier DJ, Mulroy MJ. The organization of actin filaments in the stereocilia of cochlear hair cells. *J Cell Biol*. (1980) 86:244–59. doi: 10.1083/jcb.86.1.244

4. Zheng L, Sekerkova G, Vranich K, Tilney LG, Mugnaini E, Bartles JR. The deaf jerker mouse has a mutation in the gene encoding the espin actin-bundling proteins of hair cell stereocilia and lacks espins. *Cell*. (2000) 102:377–85. doi: 10.1016/S0092-8674(00)00042-8

5. Assad JA, Shepherd GM, Corey DP. Tip-link integrity and mechanical transduction in vertebrate hair cells. *Neuron*. (1991) 7:985–94. doi: 10.1016/0896-6273(91)90343-X

6. Pickles JO, Comis SD, Osborne MP. Cross-links between stereocilia in the guinea pig organ of Corti, and their possible relation to sensory transduction. *Hear Res*. (1984) 15:103–12. doi: 10.1016/0378-5955(84)90041-8

7. Beurg M, Fettiplace R, Nam JH, Ricci AJ. Localization of inner hair cell mechanotransducer channels using high-speed calcium imaging. *Nat Neurosci*. (2009) 12:553–8. doi: 10.1038/nn.2295

8. Corey DP, Hudspeth AJ. Ionic basis of the receptor potential in a vertebrate hair cell. *Nature*. (1979) 281:675–7. doi: 10.1038/281675a0

9. Kros CJ, Rusch A, Richardson GP. Mechano-electrical transducer currents in hair cells of the cultured neonatal mouse cochlea. *Proc Biol Sci*. (1992) 249:185–93.

10. Hudspeth AJ, Corey DP. Sensitivity, polarity, and conductance change in the response of vertebrate hair cells to controlled mechanical stimuli. *Proc Natl Acad Sci USA*. (1977) 74:2407–11. doi: 10.1073/pnas.74.6.2407

11. Velez-Ortega AC, Freeman MJ, Indzhykulian AA, Grossheim JM, Frolenkov GI. Mechanotransduction current is essential for stability of the transducing stereocilia in mammalian auditory hair cells. *eLife*. (2017) 6:e24661. doi: 10.7554/eLife.24661

12. Krey JF, Chatterjee P, Dumont RA, O'sullivan M, Choi D, Bird JE, et al. Mechanotransduction-dependent control of Stereocilia dimensions and row identity in inner hair cells. *Curr Biol*. (2020) 30:442–454 e7. doi: 10.1016/j.cub.2019.11.076

13. Krey JF, Chatterjee P, Halford J, Cunningham CL, Perrin BJ, Barr-Gillespie PG. Control of stereocilia length during development of hair bundles. *PLoS Biol*. (2023) 21:e3001964. doi: 10.1371/journal.pbio.3001964

14. Mcgrath J, Tung CY, Liao X, Belyantseva IA, Roy P, Chakraborty O, et al. Actin at stereocilia tips is regulated by mechanotransduction and Adf/cofilin. *Curr Biol*. (2021) 31:1141–1153 e7. doi: 10.1016/j.cub.2020.12.006

15. Belyantseva IA, Boger ET, Friedman TB. Myosin Xva localizes to the tips of inner ear sensory cell stereocilia and is essential for staircase formation of the hair bundle. *Proc Natl Acad Sci USA*. (2003) 100:13958–63. doi: 10.1073/pnas.2334417100

16. Belyantseva IA, Boger ET, Naz S, Frolenkov GI, Sellers JR, Ahmed ZM, et al. Myosin-Xva is required for tip localization of whirlin and differential elongation of hair-cell stereocilia. *Nat Cell Biol*. (2005) 7:148–56. doi: 10.1038/ncb1219

17. Manor U, Disanza A, Grati M, Andrade L, Lin H, Di Fiore PP, et al. Regulation of stereocilia length by myosin Xva and whirlin depends on the actin-regulatory protein Eps8. *Curr Biol*. (2011) 21:167–72. doi: 10.1016/j.cub.2010.12.046

18. Tadenev ALD, Akturk A, Devanney N, Mathur PD, Clark AM, Yang J, et al. Gpsm2-Gnai specifies the tallest Stereocilia and defines hair bundle row identity. *Curr Biol*. (2019) 29:921–934 e4. doi: 10.1016/j.cub.2019.01.051

19. Mburu P, Mustapha M, Varela A, Weil D, El-Amraoui A, Holme RH, et al. Defects in whirlin, a Pdz domain molecule involved in stereocilia elongation, cause deafness in the whirler mouse and families with Dfnb31. *Nat Genet*. (2003) 34:421–8. doi: 10.1038/ng1208

20. Probst FJ, Fridell RA, Raphael Y, Saunders TL, Wang A, Liang Y, et al. Correction of deafness in shaker-2 mice by an unconventional myosin in a bac transgene. *Science*. (1998) 280:1444–7. doi: 10.1126/science.280.5368.1444

21. Liang Y, Wang A, Belyantseva IA, Anderson DW, Probst FJ, Barber TD, et al. Characterization of the human and mouse unconventional myosin xv genes responsible for hereditary deafness Dfnb3 and shaker 2. *Genomics*. (1999) 61:243–58. doi: 10.1006/geno.1999.5976

22. Ranum PT, Goodwin AT, Yoshimura H, Kolbe DL, Walls WD, Koh JY, et al. Insights into the biology of hearing and deafness revealed by single-cell Rna sequencing. *Cell Rep*. (2019) 26:3160–3171 e3. doi: 10.1016/j.celrep.2019.02.053

23. Rehman AU, Bird JE, Faridi R, Shahzad M, Shah S, Lee K, et al. Mutational Spectrum of Myo15A and the molecular mechanisms of Dfnb3 human deafness. *Hum Mutat*. (2016) 37:991–1003. doi: 10.1002/humu.23042

24. Stepanyan R, Belyantseva IA, Griffith AJ, Friedman TB, Frolenkov GI. Auditory mechanotransduction in the absence of functional myosin-Xva. *J Physiol*. (2006) 576:801–8. doi: 10.1113/jphysiol.2006.118547

25. Stepanyan R, Frolenkov GI. Fast adaptation and Ca2+ sensitivity of the mechanotransducer require myosin-Xva in inner but not outer cochlear hair cells. *J Neurosci*. (2009) 29:4023–34. doi: 10.1523/JNEUROSCI.4566-08.2009

26. Fang Q, Indzhykulian AA, Mustapha M, Riordan GP, Dolan DF, Friedman TB, et al. The 133-kDa N-terminal domain enables myosin 15 to maintain mechanotransducing stereocilia and is essential for hearing. *eLife*. (2015) 4:e08627. doi: 10.7554/eLife.08627

27. Farris HE, Leblanc CL, Goswami J, Ricci AJ. Probing the pore of the auditory hair cell mechanotransducer channel in turtle. *J Physiol*. (2004) 558:769–92. doi: 10.1113/jphysiol.2004.061267

28. Rusch A, Kros CJ, Richardson GP. Block by amiloride and its derivatives of mechano-electrical transduction in outer hair cells of mouse cochlear cultures. *J Physiol*. (1994) 474:75–86. doi: 10.1113/jphysiol.1994.sp020004

29. Hadi S, Alexander AJ, Velez-Ortega AC, Frolenkov GI. Myosin-Xva controls both staircase architecture and diameter gradation of Stereocilia rows in the auditory hair cell bundles. *J Assoc Res Otolaryngol*. (2020) 21:121–35. doi: 10.1007/s10162-020-00745-4

30. Giese APJ, Tang YQ, Sinha GP, Bowl MR, Goldring AC, Parker A, et al. Cib2 interacts with Tmc1 and Tmc2 and is essential for mechanotransduction in auditory hair cells. *Nat Commun*. (2017) 8:43. doi: 10.1038/s41467-017-00061-1

31. Ebrahim S, Avenarius MR, Grati M, Krey JF, Windsor AM, Sousa AD, et al. Stereocilia-staircase spacing is influenced by myosin iii motors and their cargos espin-1 and espin-like. *Nat Commun*. (2016) 7:10833. doi: 10.1038/ncomms10833

32. Lelli A, Michel V, Boutet De Monvel J, Cortese M, Bosch-Grau M, Aghaie A, et al. Class iii myosins shape the auditory hair bundles by limiting microvilli and stereocilia growth. *J Cell Biol*. (2016) 212:231–44. doi: 10.1083/jcb.201509017

33. López-Porras AI, Kruse AM, McClendon MT, Vélez-Ortega AC. Myosin XVA isoforms participate in the mechanotransduction-dependent remodeling of the actin cytoskeleton in auditory stereocilia. BioRxiv [Preprint]. (2024) Available at: https://www.biorxiv.org/content/10.1101/2024.09.04.611210v1